Quantum correlations in optomechanical crystals

F. Bemani,[1,*] R. Roknizadeh,[1,2,†] A. Motazedifard,[1,‡] M. H. Naderi,[1,2,§] and D. Vitali[3,4,5,‖]

[1]*Department of Physics, Faculty of Science, University of Isfahan, Hezar Jerib, 81746-73441 Isfahan, Iran*
[2]*Quantum Optics Group, Department of Physics, Faculty of Science, University of Isfahan, Hezar Jerib, 81746-73441 Isfahan, Iran*
[3]*Physics Division, School of Science and Technology, University of Camerino, I-62032 Camerino (MC), Italy*
[4]*INFN, Sezione di Perugia, via A. Pascoli, Perugia, Italy*
[5]*CNR-INO, Largo Enrico Fermi 6, I-50125 Firenze, Italy*

The field of optomechanics provides us with several examples of quantum photon-phonon interface. In this paper, we theoretically investigate the generation and manipulation of quantum correlations in a microfabricated optomechanical array. We consider a system consisting of localized photonic and phononic modes interacting locally via radiation pressure at each lattice site with the possibility of hopping of photons and phonons between neighboring sites. We show that such an interaction can correlate various modes of a driven coupled optomechanical array with well-chosen system parameters. Moreover, in the linearized regime of Gaussian fluctuations, the quantum correlations not only survive in the presence of thermal noise, but may also be generated thermally. We find that these optomechanical arrays provide a suitable platform for quantum simulation of various many-body systems.

I. INTRODUCTION

The impressive experimental progress in fabricating micromechanical and nanomechanical devices has opened a route towards the exhibition of quantum behavior at macroscopic scales. The interaction between micro- or nanomechanical oscillators and the optical field via the radiation pressure force is the basis of a wide variety of optomechanical phenomena. Despite their variety in the system sizes, parameters, and configurations, optomechanical systems (OMSs) share common features. Almost all OMSs are described by the same physics. OMSs offer further insights into the issues concerning the development of quantum memory for quantum computers [1], high-precision position, mass or force sensing [2–6], quantum transducers [7], classical and quantum communication [8], ground-state cooling of mechanical oscillators [9,10], nonclassical correlations between single photons and phonons [11], generation of nonclassical states [12], and testing of the foundations of quantum mechanics [13–16]. For a recent review and current areas of focus of quantum optomechanics see Refs. [17,18].

The extension to multimode systems is an attractive route for quantum optomechanics. A group of mechanical oscillators interacting via the radiation pressure with a common optical mode [19–26], or a group of mechanical oscillators locally interacting with a single optical mode involving the tunneling of photons and phonons between neighboring sites [27–37], are the two realizations of multimode optomechanics. The former is realized in a single optical cavity containing multiple membranes, while the latter is realized experimentally in the so-called optomechanical crystals (OMCs) in one and two dimensions.

Cooperative behaviors, emerging due to the mutual coupling, are beneficial to investigate many-body physics of photons or phonons in OMCs. An OMC is usually fabricated from a thin film of silicon membranes where an engineered defect in the crystal is used to localize an optical and a mechanical mode. OMCs usually have a large single-photon optomechanical coupling [31,38–40]. Several aspects of the array of coupled OMSs have already been investigated in the literature, involving synchronization dynamics [26–28,41,42], slowing and stopping light [32], long-range collective interactions [19], correlated quantum many-body states [28], reservoir engineering and dynamical phase transitions [25], squeezing, entanglement and state transfer between modes [33,43], transport in a one-dimensional chain [34,44,45], superradiance and collective gain [46], graphenelike Dirac physics [35], creation of artificial magnetic fields for photons on a lattice [36], quantum simulation of the propagation of the collective excitations of the photon fluid in a curved spacetime [47], and topological phases of sound and light [37].

Quantum correlations, in particular entanglement, have many applications in superdense coding, quantum teleportation [48], and protocols of quantum cryptography [49]. The generation and manipulation of entanglement in many-body systems are of great importance for quantum information processing. Furthermore, quantum correlations are valuable in characterizing various phases and corresponding quantum phase transitions in quantum many-body systems [50–52]. Bipartite entanglement plays an important role in characterizing, classifying, and simulating quantum many-body systems [53].

*foroudbemani@gmail.com
†r.roknizadeh@gmail.com
‡motazedifard.ali@gmail.com
§mhnaderi@sci.ui.ac.ir
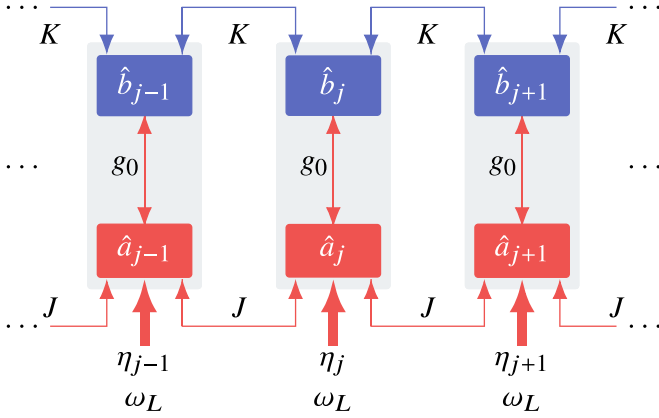‖david.vitali@unicam.it

FIG. 1. Schematic illustration of a one-dimensional OMC. Localized photonic and phononic modes couple locally via the optomechanical interaction with strength g_0 at each lattice site. Photon and phonons hop between near-neighbor sites with rates J and K, respectively. A laser at frequency ω_L and amplitude η_j drives each site.

Physical systems such as Bose-Einstein condensates [54–56], cold or thermal atoms [57,58], and trapped ions [59,60] represent promising platforms for the investigation of many-particle quantum entanglement. In the past decade, much of the attention has been devoted to entanglement in OMSs. Entanglement is one of the consequences of the coherent photon-phonon interaction in OMSs [8,61–67]. For instance, continuous-variable entanglement between two mechanical modes has recently been realized [68,69]. Since it is a possible resource for quantum technologies, quantum discord in many-body systems also requires attention.

Despite considerable efforts to understand the quantum correlations in OMSs [8,61–66,68,69], a full picture of the behavior of entanglement and of quantum discord in OMCs remains elusive. Based on the above motivations, in this paper, we consider the dynamics of coupled OMSs with a view towards quantum correlations. Employing the Heisenberg-Langevin (HL) approach and linearizing HL equations, we separate the deterministic dynamics and the quantum fluctuation dynamics. We then use HL equations to obtain the covariance matrix (CM) in order to study quantum correlations. With the CM in hand, we can investigate the degree of steady-state entanglement and the Gaussian quantum discord between different optical and mechanical modes under different conditions. We study the influence of the presence of a thermal reservoir and we show a nonmonotonic behavior of quantum correlations as a function of the heat-bath temperature.

The paper is organized as follows. In Sec. II, we begin with describing the system under consideration, i.e., an OMC. In Sec. III, we derive the HL equations of motion. We then discuss the classical equations of motion and the linearized quantum equations. In Sec. IV, we discuss the presence of entanglement and Gaussian discord in OMCs. Finally, in Sec. V, we present our concluding remarks.

II. ARRAY OF COUPLED OMSs

As depicted in Fig. 1, the system under consideration is a finite one-dimensional OMC where each site consists of a localized photonic and phononic mode coupled locally via the standard optomechanical interaction. The modes of nearby sites are connected via photon and phonon tunneling. The Hamiltonian of such a system is then given by ($\hbar = 1$) [28,34,37,44]

$$H = H_0 + H_t + H_p, \quad (1)$$

where

$$H_0 = \sum_j [\omega_c a_j^\dagger a_j + \omega_m b_j^\dagger b_j - g_0 a_j^\dagger a_j (b_j^\dagger + b_j)], \quad (2a)$$

$$H_t = -\sum_{\langle j,l \rangle} (J a_j^\dagger a_l + K b_j^\dagger b_l), \quad (2b)$$

$$H_p = \sum_j (i\eta_j e^{-i\omega_L t} a_j^\dagger - i\eta_j^* e^{i\omega_L t} a_j). \quad (2c)$$

Here, H_0 includes the free energy of each optical mode with frequency ω_c, denoted by the photon operators a_j and $a_j^\dagger$, the harmonic motion of each mechanical mode with frequency ω_m, denoted by phonon operators b_j and $b_j^\dagger$, and the usual optomechanical interaction with strength g_0. Further, H_t represents the hopping of photons and phonons between adjacent lattice sites with hopping strengths J and K, respectively. The notation $\sum_{\langle j,l \rangle}$ denotes the summation over all adjacent lattice sites. Finally, H_p denotes that each lattice site is optically driven by a laser with frequency ω_L and amplitude η_j.

III. HEISENBERG-LANGEVIN EQUATIONS

The HL equations of motion for the optical and mechanical modes in the frame rotating at the laser frequency are, respectively, given by

$$\dot{a}_j = (i\Delta - \kappa)a_j + ig_0(b_j^\dagger + b_j)a_j + iJ(a_{j-1} + a_{j+1})$$
$$+ \eta_j - \sqrt{\kappa}a_j^{\text{in}}(t), \quad (3)$$

$$\dot{b}_j = -(i\omega_m + \gamma)b_j + ig_0 a_j^\dagger a_j + iK(b_{j-1} + b_{j+1})$$
$$- \sqrt{\gamma}b_j^{\text{in}}(t), \quad (4)$$

where we have defined the laser detuning $\Delta = \omega_L - \omega_c$. In addition, κ and γ characterize, respectively, the dissipation of optical and mechanical modes. The zero-mean-value operators $a_j^{\text{in}}(t)$ and $b_j^{\text{in}}(t)$ that describe, respectively, the vacuum optical input noise and the mechanical noise operator satisfy the commutation relations

$$\left[a_j^{\text{in}}(t), a_{j'}^{\text{in},\dagger}(t')\right] = \left[b_j^{\text{in}}(t), b_{j'}^{\text{in},\dagger}(t')\right] = \delta_{jj'}\delta(t - t'), \quad (5)$$

and the Markovian correlation functions

$$\left\langle b_j^{\text{in},\dagger}(t) b_{j'}^{\text{in}}(t')\right\rangle = \bar{n}_m \delta_{jj'}\delta(t - t'), \quad (6)$$

$$\left\langle a_j^{\text{in}}(t) a_{j'}^{\text{in},\dagger}(t')\right\rangle = \delta_{jj'}\delta(t - t'), \quad (7)$$

where we have assumed that each cavity is at zero temperature and $\bar{n}_m = [\exp(\hbar\omega_m/k_B T) - 1]^{-1}$ is the mean number of thermal phonons of each mechanical mode at temperature T, with k_B being the Boltzmann constant.

A. Classical dynamics

We now employ the mean-field approximation to linearize the dynamics around the classical solutions by decomposing the quantum field operators as $a_j = \alpha_j + c_j$ and $b_j = \beta_j + d_j$, where α_j and β_j are the steady-state mean fields describing, respectively, the classical behavior of the optical and mechanical modes, and c_j and d_j are the quantum fluctuations with zero-mean value. For the aim of this paper, it is enough to consider only the translational symmetry $\alpha_j = \alpha_{j\pm1}$ and $\beta_j = \beta_{j\pm1}$, which is obtained with an approximately uniform optical driving $\eta_j \simeq \eta$, which therefore excites a background with a small wave vector $k \approx 0$. Using this assumption, the system dynamics is then simplified to the single-site case. The equations of motion for the steady-state classical mean fields can be obtained by averaging Eqs. (3) and (4) over classical and quantum fluctuations,

$$\alpha_j = \alpha \simeq \frac{i\eta}{(\Delta + i\kappa + 2J + 2g_0\mathrm{Re}\beta)}, \qquad (8)$$

$$\beta_j = \beta \simeq \frac{g_0|\alpha|^2}{(\omega_m - i\gamma - 2K)}, \qquad (9)$$

where Re denotes the real part.

B. Linearized quantum dynamics

We study the quantum statistical properties of the system through the small fluctuations of the operators around the steady-state classical mean values given by Eqs. (8) and (9). Using the standard definition of the optical and mechanical mode quadratures $X_j = (c_j + c_j^\dagger)/\sqrt{2}$, $Y_j = (c_j - c_j^\dagger)/i\sqrt{2}$, $x_j = (d_j + d_j^\dagger)/\sqrt{2}$, and $y_j = (d_j - d_j^\dagger)/i\sqrt{2}$, the equations of motion for the quantum fluctuations are

given by

$$\dot{X}_j = -(\Delta + 2g_0\mathrm{Re}\beta)Y_j - \kappa X_j - 2g_0\mathrm{Im}\alpha x_j \\ -J(Y_{j-1} + Y_{j+1}) - \sqrt{\kappa}X_j^{\mathrm{in}}(t), \qquad (10)$$

$$\dot{Y}_j = (\Delta + 2g_0\mathrm{Re}\beta)X_j - \kappa Y_j + 2g_0\mathrm{Re}\alpha x_j \\ +J(X_{j-1} + X_{j+1}) - \sqrt{\kappa}Y_j^{\mathrm{in}}, \qquad (11)$$

$$\dot{x}_j = -\gamma x_j + \omega_m y_j - K(y_{j-1} + y_{j+1}) - \sqrt{\gamma}x_j^{\mathrm{in}}, \quad (12)$$

$$\dot{y}_j = -\omega_m x_j - \gamma y_j + 2g_0(\mathrm{Re}\alpha X_j + \mathrm{Im}\alpha Y_j) \\ +K(x_{j-1} + x_{j+1}) - \sqrt{\gamma}y_j^{\mathrm{in}}, \qquad (13)$$

where Im denotes the imaginary part. We now express the linearized HL equations in the following compact matrix form:

$$\dot{\mathbf{u}}(t) = \mathbf{A}\mathbf{u}(t) + \mathbf{n}(t), \qquad (14)$$

where we have defined the vector of fluctuation operators $\mathbf{u} = [\cdots \mathbf{v}_{j-1}, \mathbf{v}_j, \mathbf{v}_{j+1}, \cdots]^T$ with $\mathbf{v}_j = [X_j, Y_j, x_j, y_j]$ and the corresponding vector of noises $\mathbf{n} = [\cdots \mathbf{m}_{j-1}, \mathbf{m}_j, \mathbf{m}_{j+1}, \cdots]^T$ with $\mathbf{m}_j = [\sqrt{\kappa}X_j^{\mathrm{in}}, \sqrt{\kappa}Y_j^{\mathrm{in}}, \sqrt{\gamma}x_j^{\mathrm{in}}, \sqrt{\gamma}y_j^{\mathrm{in}}]$, in which $X_j^{\mathrm{in}} = (a_j^{\mathrm{in}} + a_j^{\dagger,\mathrm{in}})/\sqrt{2}$, $Y_j^{\mathrm{in}} = (a_j^{\mathrm{in}} - a_j^{\dagger,\mathrm{in}})/i\sqrt{2}$, $x_j^{\mathrm{in}} = (b_j^{\mathrm{in}} + b_j^{\dagger,\mathrm{in}})/\sqrt{2}$, and $y_j^{\mathrm{in}} = (b_j^{\mathrm{in}} - b_j^{\dagger,\mathrm{in}})/i\sqrt{2}$ are the input noise quadratures of the optical and mechanical modes. Furthermore, we define the drift matrix $\mathbf{A}$ as

$$\mathbf{A} = \begin{bmatrix} \ddots & \ddots & 0 & 0 & 0 \\ \ddots & \mathbf{B} & \mathbf{C} & 0 & 0 \\ 0 & \mathbf{C} & \mathbf{B} & \mathbf{C} & 0 \\ 0 & 0 & \mathbf{C} & \mathbf{B} & \ddots \\ 0 & 0 & 0 & \ddots & \ddots \end{bmatrix}, \qquad (15)$$

with the blocks

$$\mathbf{B} = \begin{bmatrix} -\kappa & -(\Delta + 2g_0\mathrm{Re}\beta) & -2g_0\mathrm{Im}\alpha & 0 \\ (\Delta + 2g_0\mathrm{Re}\beta) & -\kappa & 2g_0\mathrm{Re}\alpha & 0 \\ 0 & 0 & -\gamma & \omega_m \\ 2g_0\mathrm{Re}\alpha & 2g_0\mathrm{Im}\alpha & -\omega_m & -\gamma \end{bmatrix}, \qquad (16)$$

$$\mathbf{C} = \begin{bmatrix} 0 & -J & 0 & 0 \\ J & 0 & 0 & 0 \\ 0 & 0 & 0 & -K \\ 0 & 0 & K & 0 \end{bmatrix}. \qquad (17)$$

IV. STEADY-STATE QUANTUM CORRELATIONS

Due to the Gaussian nature of the quantum noises and to the linearized dynamics, the steady state of the quantum fluctuations of the OMCs is a continuous-variable $2N$-partite Gaussian state, which is completely determined by its $4N \times 4N$ CM. The formal solution of Eq. (14) is

$$\mathbf{u}(t) = \mathbf{M}(t)\mathbf{u}(0) + \int_0^t \mathbf{M}(t-s)\mathbf{n}(s)ds, \qquad (18)$$

with $\mathbf{M}(t) = \exp[t\mathbf{A}]$. The CM defined as

$$\mathbf{V}_{pq}(t) = \frac{1}{2}\langle \mathbf{u}_p(t)\mathbf{u}_q(t) + \mathbf{u}_q(t)\mathbf{u}_p(t) \rangle \qquad (19)$$

contains all information about the quantum correlation between various mechanical and optical modes where $\mathbf{u}_p(t)$ is the pth component of the vector $\mathbf{u}(t)$.

The system reaches its steady state when $\mathbf{M}(\infty) = 0$. Our analysis is restricted to the stable regime where all the eigenvalues of the drift matrix have negative real parts. In Fig. 2, we plot the region of stability as a function of the
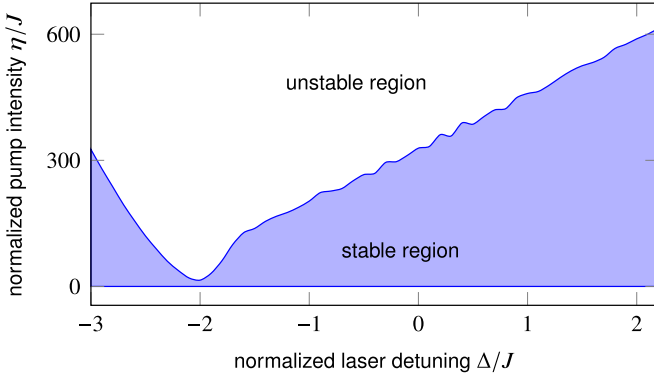
FIG. 2. Stability domain as a function of the normalized input power η/J and normalized detuning Δ/J. The white and blue areas correspond to the unstable and stable correlated regimes, respectively. The normalized parameters are set with respect to J, $\kappa/J = 0.1$, $g_0/J = 10^{-4}$, $\gamma/J = 0.002$, $\omega_m/J = 0.1$, and $K/J = 0.05$. Temperatures of the photonic and phononic heat baths are considered to be zero.

normalized laser pump intensity and detuning. For large laser drive, the system enters the unstable region. In the steady state, one gets the CM elements as

$$\mathbf{V}_{ij} = \sum_{k,l} \int_0^\infty ds \int_0^\infty ds' \mathbf{M}_{ik}(s) \mathbf{M}_{jl}(s') \Phi_{kl}(s - s'), \quad (20)$$

where

$$\Phi_{kl}(s) = \frac{1}{2} \langle \mathbf{n}_k(s) \mathbf{n}_l(s') + \mathbf{n}_l(s') \mathbf{n}_k(s) \rangle$$
$$= \mathbf{D}_{kl} \delta(s - s'), \quad (21)$$

where $\mathbf{D} = \text{diag}[\cdots \mathbf{F}, \mathbf{F}, \mathbf{F}, \cdots]^T$ with $\mathbf{F} = \text{diag} [\kappa, \kappa, \gamma(2\bar{n}_m + 1), \gamma(2\bar{n}_m + 1)]$. When the stability conditions are satisfied so that $\mathbf{M}(\infty) = 0$, the steady-state CM, $\mathbf{V}$, can be obtained by solving the linearized HL Eq. (14) for the quantum fluctuations, which fulfill the following Lyapunov equation:

$$\mathbf{A}\mathbf{V} + \mathbf{V}\mathbf{A}^T = -\mathbf{D}. \quad (22)$$

With these classical and quantum steady-state solutions in hand, we next employ the CM formalism to calculate the steady-state quantum correlations. We check the presence of the quantum correlations between the mechanical and optical modes on the same site, as well as between the mechanical or optical modes with different site indices. Considering the following reduced CM of the two modes:

$$\mathbf{V}_R = \begin{bmatrix} \mathbf{V}_A & \mathbf{V}_C \\ \mathbf{V}_C^T & \mathbf{V}_B \end{bmatrix}, \quad (23)$$

one can calculate the quantum correlations. Here, $\mathbf{V}_A$, $\mathbf{V}_B$, and $\mathbf{V}_C$ are 2×2 matrices where $\mathbf{V}_A$ and $\mathbf{V}_B$ account for the local properties of modes A and B, respectively, while $\mathbf{V}_C$ describes intermode correlations. A and B may stand for two different modes.

A. Steady-state entanglement

We quantify the degree of entanglement in terms of the logarithmic negativity, which is an entanglement mono-
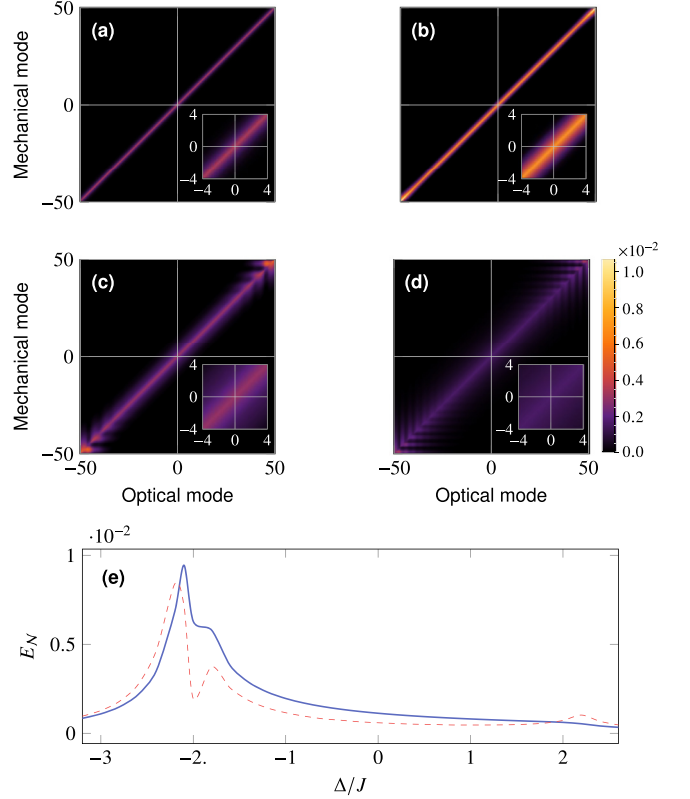

FIG. 3. The degree of entanglement between optical and mechanical modes in terms of the logarithmic negativity for various values of the laser detuning: (a) $\Delta/J = -2.5$, (b) $\Delta/J = -2.1$, (c) $\Delta/J = -1.7$, and (d) $\Delta/J = -1.3$ for 101 coupled OMSs. (e) The logarithmic negativity between the two optical and mechanical modes with the same site index $j = -50$ or $j = 50$ (blue solid line) and $j = 0$ (red dashed line) vs the laser detuning. We set normalized parameters with respect to J, $\kappa/J = 0.1$, $\eta/J = 15$, $g_0/J = 10^{-4}$, $\gamma/J = 0.002$, $\omega_m/J = 0.1$, and $K/J = 0.05$. Temperatures of the photonic and phononic heat baths are considered to be zero.

tone, and it is given by $E_N = \max\{0, -\ln 2\tilde{\nu}_-\}$ with $\tilde{\nu}_- = 2^{-1/2}(\Sigma_- - \sqrt{\Sigma_-^2 - 4 \det \mathbf{V}_R})^{1/2}$ being the smallest of the two symplectic eigenvalues of the partially transposed CM and $\Sigma_\pm = \det \mathbf{V}_A + \det \mathbf{V}_B \pm 2 \det \mathbf{V}_C$.

1. Photon-phonon entanglement

The degree of entanglement between optical and mechanical modes in terms of the logarithmic negativity for various laser detuning at zero temperature of both the photonic and phononic heat baths is shown in Figs. 3(a)–3(d). We can see that one has mostly on-site optomechanical entanglement, i.e., between modes at the same sites, and that there is no long-range photon-phonon entanglement. However, as suggested by the zoomed insets, one has that due to the combined action of the on-site optomechanical interaction and of tunneling of the photons and phonons between lattice sites, there is some amount of off-site entanglement between the optical and mechanical modes. For instance, the optical mode at site $j = 0$ is entangled with the neighbor mechanical modes at sites $|j| < 1$, $|j| < 2$, $|j| < 3$, and $|j| < 4$ for $\Delta/J = -2.5$, $\Delta/J =$
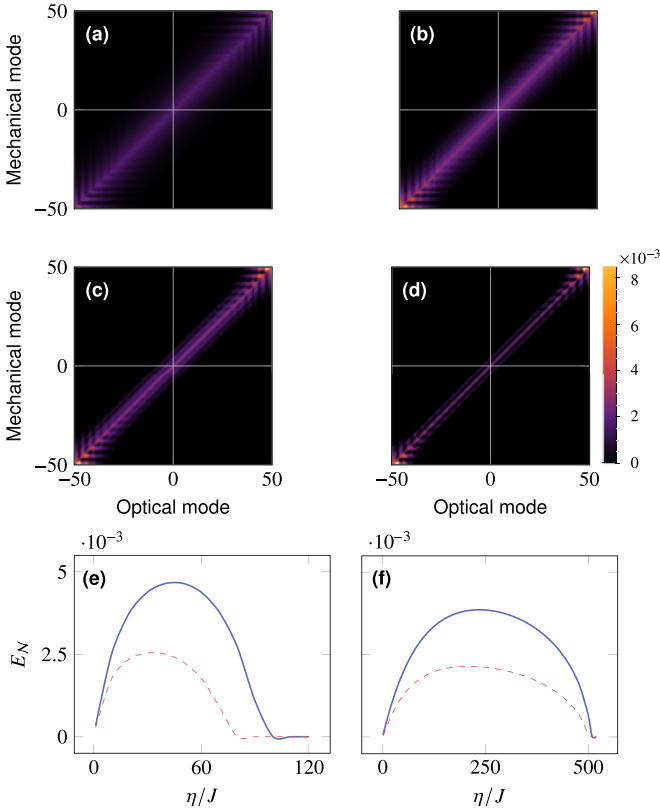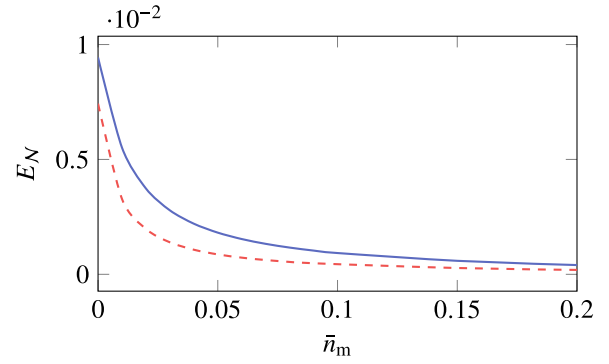
FIG. 5. Steady-state photon-phonon entanglement for the site index $j = -50$ or $j = 50$ vs the thermal phonon number $\bar{n}_m$ for two values of the normalized laser detuning $\Delta/J = -2$ (red dashed line) and $\Delta/J = -2.1$ (blue solid line) for 101 coupled OMSs. Here, we consider mechanical resonators with frequency $\omega_m/2\pi = 9$ GHz and the other parameters are the same as in Fig. 3.

FIG. 4. The degree of entanglement between optical and mechanical modes in terms of the logarithmic negativity for various values of the laser intensity: (a) $\eta/J = 50$, (b) $\eta/J = 150$, (c) $\eta/J = 250$, and (d) $\eta/J = 350$ for 101 coupled OMSs. We set $\Delta/J = 1.5$, and other parameters are the same as Fig. 3. (e), (f) The logarithmic negativity between the two optical and mechanical modes with the same index $j = -50$ or $j = 50$ (blue solid line) and $j = 0$ (red dashed line) vs the normalized laser pump intensity for two values of the laser detuning: (e) $\Delta/J = -1.5$ and (f) $\Delta/J = 1.5$.

-2.1, $\Delta/J = -1.7$, and $\Delta/J = -1.3$. It is also evident that the detuning has a significant effect on the optomechanical entanglement. We address this issue in Fig. 3(e), where we have plotted the logarithmic negativity between the two optical and mechanical modes with the same site index $j = -50$ or $j = 50$ and $j = 0$ versus the laser detuning.

Our choices for the detuning and laser pump intensity correspond to the stable region of Fig. 2. Furthermore, since we did not consider the periodic boundary conditions, one can see a nonuniform behavior at the lattice edges.

In Figs. 4(a)–4(d), we show how the photon-phonon entanglement varies as a function of the laser pump intensity for a fixed laser detuning, $\Delta/J = 1.5$. By increasing the laser intensity, the entanglement first tends to increase and then to decrease as we approach the unstable region. Therefore, there is a nonmonotonic behavior of on-site entanglement. We show this fact in Figs 4(e) and 4(f), where we have plotted the logarithmic negativity between the two optical and mechanical modes with the same site index at the lattice edge ($j = -50$ or 50) and at the lattice center ($j = 0$) versus the

normalized laser pump intensity for two values of the laser detuning.

Finally, we have also studied the eventual presence of photon-photon or phonon-phonon entanglement between different sites. We have verified that for all choices of the parameters, this kind of intersite entanglement is always zero.

2. Thermal effects on the generated entanglement

Usually, quantum correlations and entanglement in particular are fragile with respect to thermal noise. Therefore, the investigation of the effect of thermal fluctuations on the bipartite quantum correlations in OMCs is of particular relevance for applications.

In Fig. 5, we show how the on-site photon-phonon entanglement changes with increasing thermal phonon number $\bar{n}_m$. Evidently, the on-site photon-phonon entanglement decays for increasing temperatures and it persists at ultracryogenic temperatures achievable in dilution refrigerators (for example, $\bar{n}_m \simeq 0.06$ for mechanical resonance frequency $\omega_m/2\pi = 9$ GHz at a temperature of $T = 0.15$ K).

B. Steady-state Gaussian quantum discord

It is also interesting to examine if quantum discord [70,71], a measure of the quantumness of correlations, is present in the steady state of the system. The Gaussian quantum discord is an asymmetric quantity and the Gaussian quantum A-discord of the Gaussian state of two modes, A and B, is given by [72,73]

$$\mathfrak{D}^{\rightarrow} = f(\sqrt{\beta}) - f(\upsilon_-) - f(\upsilon_+) - f(\sqrt{\varepsilon}), \qquad (24)$$

where

$$f(x) = \left(\frac{x+1}{2}\right)\log_{10}\left(\frac{x+1}{2}\right) - \left(\frac{x-1}{2}\right)\log_{10}\left(\frac{x-1}{2}\right), \qquad (25)$$

$$\upsilon_\pm = \sqrt{\frac{\Sigma_+ \pm \sqrt{\Sigma_+^2 - 4\det \mathbf{V}_R}}{2}} \qquad (26)$$
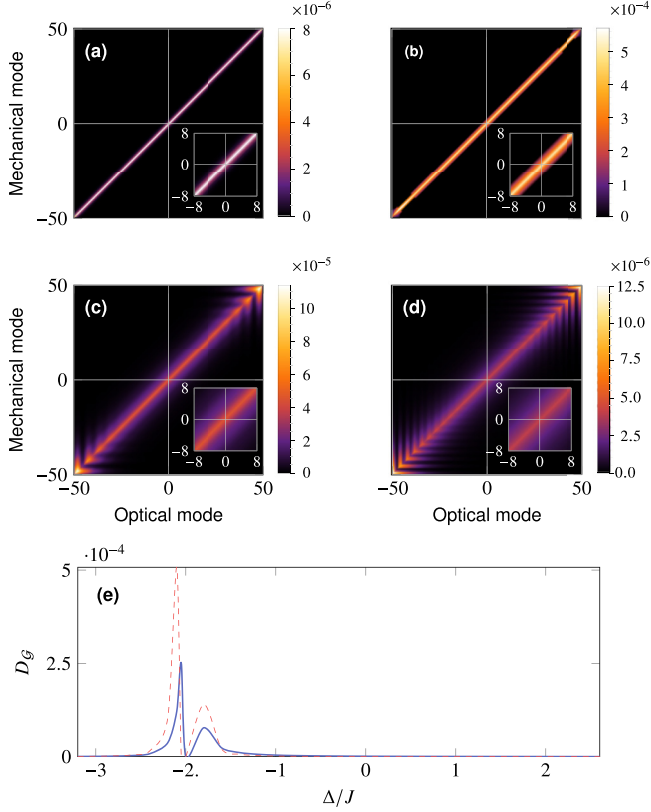
FIG. 6. Steady-state symmetrized Gaussian quantum discord between optical and mechanical modes for various laser detuning values: (a) $\Delta/J = -2.5$, (b) $\Delta/J = -2.1$, (c) $\Delta/J = -1.7$, and (d) $\Delta/J = -1.3$ for 101 coupled OMSs. (e) The symmetrized Gaussian quantum discord between the two optical and mechanical modes with the same index $j = 0$ (blue solid line) and $j = 50$ (red dashed line) vs the laser detuning. The heat-bath temperatures for mechanical and optical modes are considered to be zero. Other parameters are the same as Fig. 3.

FIG. 7. Steady-state Gaussian quantum discord between optical and mechanical modes for various laser intensity values: (a) $\eta/J = 50$, (b) $\eta/J = 200$, (c) $\eta/J = 350$, and (d) $\eta/J = 500$ for 101 coupled OMSs. Here, we set $\Delta/J = 1.5$, and other parameters are the same as Fig. 3. (e), (f) The steady-state Gaussian quantum discord between the two optical and mechanical modes with the same site index $j = 50$ or $j = -50$ (red dashed line) and $j = 0$ (blue solid line) vs the normalized laser pump intensity for two values of the laser detuning: (e) $\Delta/J = -1.5$ and (f) $\Delta/J = 1.5$.

are the two symplectic eigenvalues of the two-mode CM and

$$
\varepsilon = \begin{cases} \dfrac{2\gamma^2 + (\beta-1)(\delta-\alpha) + 2|\gamma|\sqrt{\gamma^2 + (\beta-1)(\delta-\alpha)}}{(\beta-1)^2}, & \dfrac{(\delta-\alpha\beta)^2}{(\beta+1)\gamma^2(\alpha+\delta)} \leqslant 1 \\[4mm] \dfrac{\alpha\beta - \gamma^2 + \delta - \sqrt{\gamma^4 + (\delta-\alpha\beta)^2 - 2\gamma^2(\delta+\alpha\beta)}}{2\beta}, & \text{otherwise,} \end{cases}
$$

(27)

where $\alpha = \det\mathbf{V}_A$, $\beta = \det\mathbf{V}_B$, $\gamma = \det\mathbf{V}_C$, and $\delta = \det\mathbf{V}_R$ are the symplectic invariants. One can obtain the Gaussian quantum B-discord $\mathfrak{D}^{\leftarrow}$ by swapping the roles of the two modes, A and B, which is equivalent to swapping α and β in the above formulas. Since we are interested in quantum correlations in general between the different modes in the one-dimensional array, from now on we will consider the symmetrized quantum discord, $D_{\mathcal{G}} = \max\{\mathfrak{D}^{\leftarrow}, \mathfrak{D}^{\rightarrow}\}$.

1. Photon-phonon steady-state Gaussian quantum discord

Figure 6 shows the behavior of the symmetrized quantum discord $D_{\mathcal{G}}$ for various laser detuning values at zero temperature of both photonic and phononic modes. Similarly to what occurred for entanglement, changing the laser detuning has a significant effect on the photon-phonon Gaussian quantum discord, and again we have a similar behavior with that of
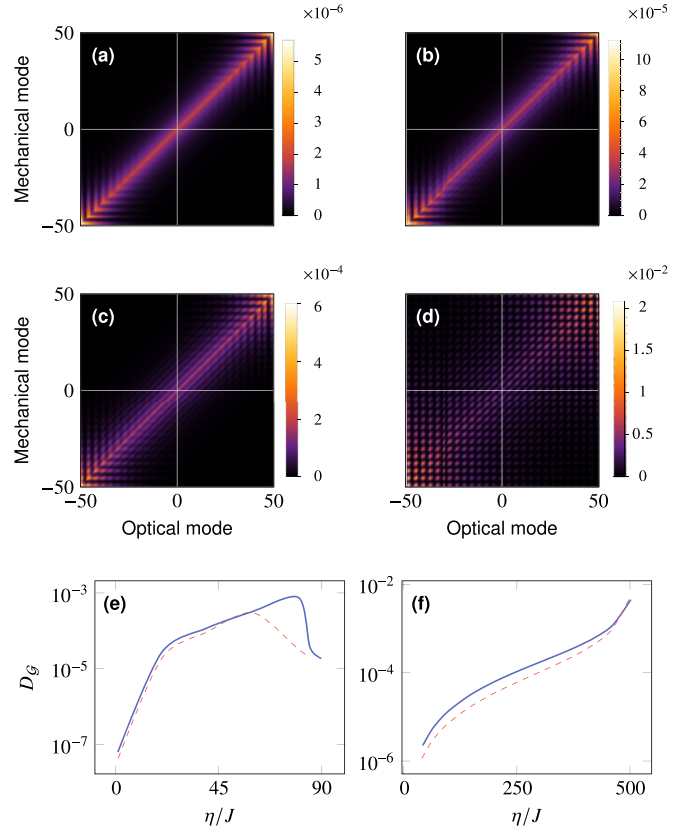
entanglement with the above choice of parameters, with the presence of larger on-site discord between the mechanical and the optical mode and which extends for few sites. One starts to see a different behavior between Gaussian discord and entanglement when looking at the dependence upon the driving power and specifically if we consider increasing values of the laser drive η. In Fig. 7, we show how steady-state photon-phonon Gaussian quantum discord varies with the laser intensity for a fixed laser detuning, $\Delta/J = 1.5$. In contrast to the behavior of entanglement, we have that by increasing the laser intensity, one has a significant increase of Gaussian quantum discord between optical and mechanical sites [see Figs. 7(e) and 7(f)]. Moreover, at larger values, one can see a long-range correlation between optical and mechanical modes appearing [see Fig. 7(d)].

2. Photon-photon and phonon-phonon steady-state Gaussian quantum discord

The appearance of long-range quantum correlations also occurs when considering either only optical modes or only mechanical modes, at each site of the OMC, in clear contrast
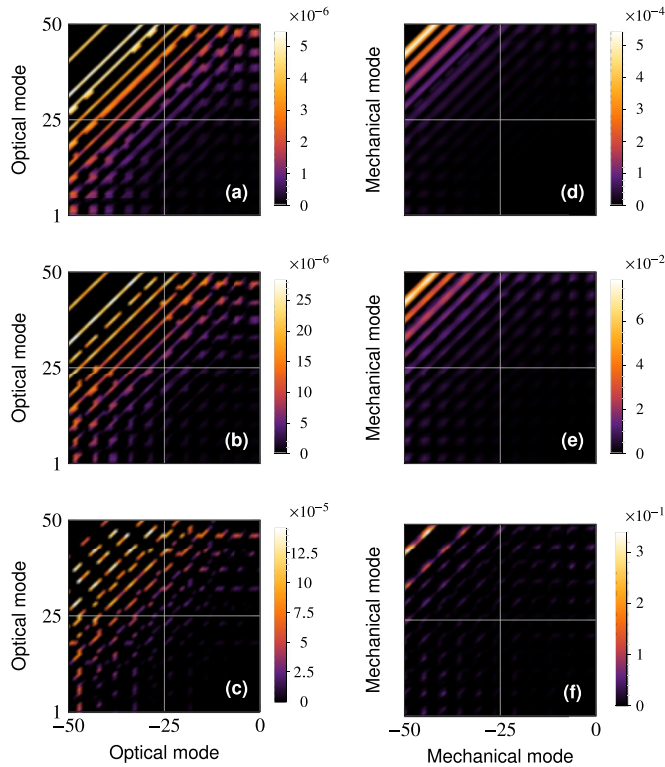
FIG. 8. Steady-state Gaussian quantum discord between (a)–(c) optical modes and (e), (f) mechanical modes for various values of the laser intensity: (a), (d) $\eta/J = 80$, (b), (e) $\eta/J = 100$, and (c), (f) $\eta/J = 120$ for 101 coupled OMSs. The normalized laser detuning is set to $\Delta/J = -1.5$. Other parameters are the same as Fig. 2.

FIG. 9. Steady-state Gaussian quantum discord under different heat-bath phonon number for normalized laser detuning $\Delta/J = 1.5$, driving $\eta/J = 500$, and mechanical resonance frequency $\omega_m/2\pi = 9$ GHz: (a) $\bar{n}_m = 0.1$ ($T = 0.18$ K), (b) $\bar{n}_m = 0.5$ ($T = 0.39$ K), (c) $\bar{n}_m = 2.5$ ($T = 1.28$ K), and (d) $\bar{n}_m = 12.5$ ($T = 5.59$ K) for 101 coupled OMSs. Legend bar is the same for (a)–(c). Parameters are the same as Fig. 2. See Fig. 7(d) for zero heat-bath temperature. (e) The steady-state Gaussian quantum discord between the two optical and mechanical modes with the same site index $j = 50$ or $j = -50$ (red dashed line), $j = 0$ (blue solid line), and with the different site index $j = 0$ and $j = 50$ (green dotted line) vs heat-bath phonon number.

to the case of entanglement which is instead completely absent, even between neighboring sites. This fact is shown in Fig. 8. As can bee seen, for a fixed laser detuning, by increasing the laser intensity the steady-state Gaussian quantum discord between modes of the same nature increases.

3. Thermal effects on the steady-state Gaussian quantum discord

It is relevant to study the robustness of the Gaussian quantum discord with respect to temperature as we did already for entanglement. The steady-state Gaussian quantum discord under different heat-bath phonon number for normalized laser detuning $\Delta/J = 1.5$ and laser intensity $\eta/J = 500$ is depicted in Fig. 9. One can see a nonmonotonic behavior in Gaussian quantum discord by increasing the thermal phonon number. It first tends to increase, then decreases, and finally increases again. This behavior is somewhat unexpected and it can be regarded as evidence of thermally induced Gaussian quantum discord in OMCs. This is not completely novel, however, in quantum many-body systems; for instance, the transverse-field XY model also shows nonmonotonic behavior of its quantum correlations (for instance, see [74] and references therein). We remark, however, that our model is not exactly the same as the XY model regarding the effects of the thermal environment because, in the latter, the involved excitations have similar frequencies and therefore similar thermal effects, while in our case, due to the large difference in frequencies between optical and mechanical modes, only the phonon
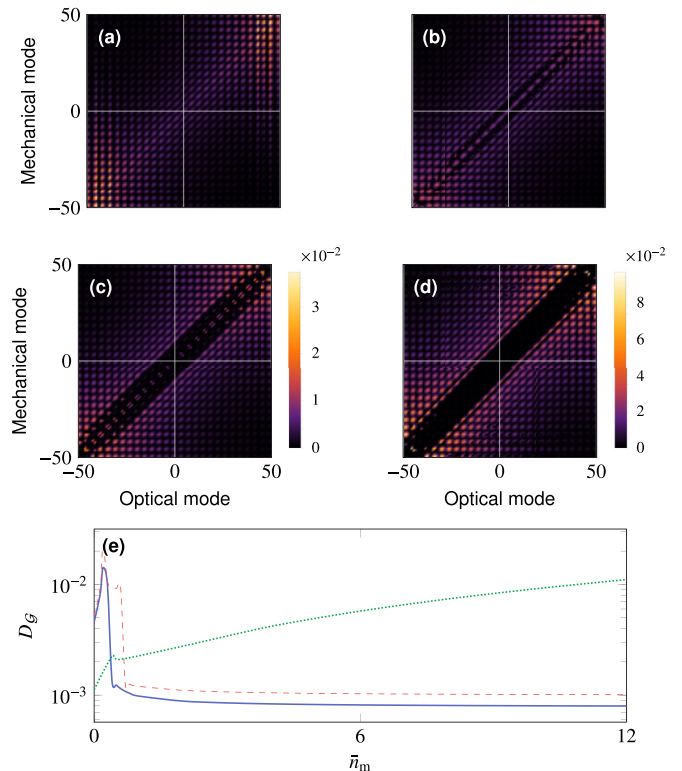
modes are appreciably affected by a nonzero reservoir temperature. The phenomenon investigated here instead shares some similarity with what has already been underlined in [75,76], where it has been shown that for continuous-variable bipartite systems, quantum discord can increase for increasing thermal noise because they represent nonclassical correlations which are induced and maintained thanks to the mediating action of the local dissipative bath.

V. CONCLUSIONS

In conclusion, our investigation clearly demonstrates the presence of appreciable quantum correlations in an OMC where each site consists of two localized, i.e., optical and mechanical, modes coupled locally via the optomechanical interaction. The modes of nearby sites are connected via both photon and phonon tunneling. In particular, the generation of on-site or short-range entanglement between optical and mechanical modes that rely on the optomechanical interactions in OMCs seems feasible at ultracryogenic temperatures. The generated entanglement is very fragile with respect to thermal noise. We have also shown that there is no long-range

entanglement between optical and mechanical modes. Moreover, there is no photon-photon or phonon-phonon entanglement in the system. Regarding the absence of strong entanglement between modes of the same nature, this is due to the quantum dynamics realized by the chosen model Hamiltonian. In fact, it does not contain terms of the form of $a_j^\dagger a_{j\pm1}^\dagger + a_j a_{j\pm1}$ for the photonic modes (or $b_j^\dagger b_{j\pm1}^\dagger + b_j b_{j\pm1}$ for phononic modes). It only contains hopping terms, which cannot directly entangle modes of the same nature.

We have then examined a weaker form of quantum correlation, i.e., Gaussian quantum discord, and we have studied if quantum discord is present in the steady state of the system for various control parameters. The Gaussian quantum discord behavior is completely different; one has long-range features in all three possible cases of correlations, i.e., photon-phonon, photon-photon, and phonon-phonon cases, at variance with what occurs with entanglement. A further interesting aspect is the thermal activation of quantum discord, i.e., the fact that photon-phonon discord *increases* with increasing temperature. In our opinion, this is a manifestation of the transfer of nonclassical correlations mediated by the thermal reservoir, as already discussed for continuous-variable systems in [75,76].

The present study, which paves the way toward the investigation of many-body entanglement, can be considered as a step toward controlled quantum correlations between different quantum processors across the lattice sites, with potential applications in quantum information processing and storage. The proposed scheme also provides a suitable platform for quantum simulation of various many-body systems with optomechanical crystals by tuning the system parameters.

It should be noted that we did not consider the disorder effect in our study. As an outlook, the system under consideration can be generalized to a more realistic case where the lattice disorder is also present in the system. Another outlook may be the generalization to the case of two-dimensional lattices of coupled optomechanical systems.

ACKNOWLEDGMENTS

[1] G. D. Cole and M. Aspelmeyer, Cavity optomechanics: Mechanical memory sees the light, Nat. Nanotechnol. **6**, 690 (2011).

[2] A. G. Krause, M. Winger, T. D. Blasius, Q. Lin, and O. Painter, A high-resolution microchip optomechanical accelerometer, Nat. Photon. **6**, 768 (2012).

[3] A. Motazedifard, F. Bemani, M. H. Naderi, R. Roknizadeh, and D. Vitali, Force sensing based on coherent quantum noise cancellation in a hybrid optomechanical cavity with squeezed-vacuum injection, New J. Phys. **18**, 073040 (2016).

[4] K. W. Murch, K. L. Moore, S. Gupta, and D. M. Stamper-kurn, Observation of quantum-measurement backaction with an ultracold atomic gas, Nat. Phy. **4**, 561 (2008).

[5] T. P. Purdy, R. W. Peterson, and C. Regal, Observation of radiation pressure shot noise on a macroscopic object, Science **339**, 801 (2013).

[6] J. Chaste, A. Eichler, J. Moser, G. Ceballos, R. Rurali, and A. Bachtold, A nanomechanical mass sensor with yoctogram resolution, Nat. Nanotechnol. **7**, 301 (2012).

[7] J. Bochmann, A. Vainsencher, D. D. Awschalom, and A. N. Cleland, Nanomechanical coupling between microwave and optical photons, Nat. Phys. **9**, 712 (2013).

[8] T. Palomaki, J. Harlow, J. Teufel, R. Simmonds, and K. Lehnert, Coherent state transfer between itinerant microwave fields and a mechanical oscillator, Nature (London) **495**, 210 (2013).

[9] J. Chan, T. M. Alegre, A. H. Safavi-Naeini, J. T. Hill, A. Krause, S. Gröblacher, M. Aspelmeyer, and O. Painter, Laser cooling of a nanomechanical oscillator into its quantum ground state, Nature (London) **478**, 89 (2011).

[10] J. Teufel, T. Donner, D. Li, J. Harlow, M. Allman, K. Cicak, A. Sirois, J. Whittaker, K. Lehnert, and R. Simmonds, Sideband cooling of micromechanical motion to the quantum ground state, Nature (London) **475**, 359 (2011).

[11] R. Riedinger, S. Hong, R. Norte, J. Slater, J. Shang, A. Krause, V. Anant, M. Aspelmeyer, and S. Gröblacher, Nonclassical correlations between single photons and phonons from a mechanical oscillator, Nature (London) **530**, 313 (2016).

[12] D. W. Brooks, T. Botter, S. Schreppler, T. P. Purdy, N. Brahms, and D. M. Stamper-Kurn, Nonclassical light generated by quantum-noise-driven cavity optomechanics, Nature (London) **488**, 476 (2012).

[13] M. Bawaj, C. Biancofiore, M. Bonaldi, F. Bonfigli, A. Borrielli, G. Di Giuseppe, L. Marconi, F. Marino, R. Natali, A. Pontin *et al.*, Probing deformed commutators with macroscopic harmonic oscillators, Nat. Commun. **6**, 7503 (2015).

[14] I. Pikovski, M. R. Vanner, M. Aspelmeyer, M. Kim, and C. Brukner, Probing planck-scale physics with quantum optics, Nat. Phys. **8**, 393 (2012).

[15] V. C. Vivoli, T. Barnea, C. Galland, and N. Sangouard, Proposal for an Optomechanical Bell Test, Phys. Rev. Lett. **116**, 070405 (2016).

[16] I. Marinković, A. Wallucks, R. Riedinger, S. Hong, M. Aspelmeyer, and S. Gröblacher, Optomechanical Bell Test, Phys. Rev. Lett. **121**, 220404 (2018).

[17] M. Aspelmeyer, T. J. Kippenberg, and F. Marquardt, Cavity optomechanics, Rev. Mod. Phys. **86**, 1391 (2014).

[18] W. P. Bowen and G. J. Milburn, *Quantum Optomechanics* (CRC, Boca Raton, FL, 2015).

[19] A. Xuereb, C. Genes, and A. Dantan, Strong Coupling and Long-Range Collective Interactions in Optomechanical Arrays, Phys. Rev. Lett. **109**, 223601 (2012).

[20] C. A. Holmes, C. P. Meaney, and G. J. Milburn, Synchronization of many nanomechanical resonators coupled via a common cavity field, Phys. Rev. E **85**, 066203 (2012).

[21] A. Xuereb, C. Genes, and A. Dantan, Collectively enhanced optomechanical coupling in periodic arrays of scatterers, Phys. Rev. A **88**, 053803 (2013).

[22] A. Xuereb, C. Genes, G. Pupillo, M. Paternostro, and A. Dantan, Reconfigurable Long-Range Phonon Dynamics in Optomechanical Arrays, Phys. Rev. Lett. **112**, 133604 (2014).

[23] H. Seok, L. F. Buchmann, E. M. Wright, and P. Meystre, Multimode strong-coupling quantum optomechanics, Phys. Rev. A **88**, 063850 (2013).

[24] M. Bhattacharya and P. Meystre, Multiple membrane cavity optomechanics, Phys. Rev. A **78**, 041801(R) (2008).

[25] A. Tomadin, S. Diehl, M. D. Lukin, P. Rabl, and P. Zoller, Reservoir engineering and dynamical phase transitions in optomechanical arrays, Phys. Rev. A **86**, 033821 (2012).

[26] F. Bemani, A. Motazedifard, R. Roknizadeh, M. H. Naderi, and D. Vitali, Synchronization dynamics of two nanomechanical membranes within a Fabry-Perot cavity, Phys. Rev. A **96**, 023805 (2017).

[27] G. Heinrich, M. Ludwig, J. Qian, B. Kubala, and F. Marquardt, Collective Dynamics in Optomechanical Arrays, Phys. Rev. Lett. **107**, 043603 (2011).

[28] M. Ludwig and F. Marquardt, Quantum Many-Body Dynamics in Optomechanical Arrays, Phys. Rev. Lett. **111**, 073603 (2013).

[29] A. H. Safavi-Naeini and O. Painter, Proposal for an optomechanical traveling wave phonon-photon translator, New J. Phys. **13**, 013017 (2011).

[30] J. Chan, A. H. Safavi-Naeini, J. T. Hill, S. Meenehan, and O. Painter, Optimized optomechanical crystal cavity with acoustic radiation shield, Appl. Phys. Lett. **101**, 081115 (2012).

[31] A. H. Safavi-Naeini, J. T. Hill, S. Meenehan, J. Chan, S. Gröblacher, and O. Painter, Two-dimensional phononic-photonic band gap optomechanical crystal cavity, Phys. Rev. Lett. **112**, 153603 (2014).

[32] D. E. Chang, A. H. Safavi-Naeini, M. Hafezi, and O. Painter, Slowing and stopping light using an optomechanical crystal array, New J. Phys. **13**, 023003 (2011).

[33] M. Schmidt, M. Ludwig, and F. Marquardt, Optomechanical circuits for nanomechanical continuous variable quantum state processing, New J. Phys. **14**, 125005 (2012).

[34] W. Chen and A. A. Clerk, Photon propagation in a one-dimensional optomechanical lattice, Phys. Rev. A **89**, 033854 (2014).

[35] M. Schmidt, V. Peano, and F. Marquardt, Optomechanical Dirac physics, New J. Phys. **17**, 023025 (2015).

[36] M. Schmidt, S. Kessler, V. Peano, O. Painter, and F. Marquardt, Optomechanical creation of magnetic fields for photons on a lattice, Optica **2**, 635 (2015).

[37] V. Peano, C. Brendel, M. Schmidt, and F. Marquardt, Topological Phases of Sound and Light, Phys. Rev. X **5**, 031011 (2015).

[38] M. Eichenfield, J. Chan, R. M. Camacho, K. J. Vahala, and O. Painter, Optomechanical crystals, Nature (London) **462**, 78 (2009).

[39] A. H. Safavi-Naeini, T. P. M. Alegre, M. Winger, and O. Painter, Optomechanics in an ultrahigh-Q two-dimensional photonic crystal cavity, Appl. Phys. Lett. **97**, 181106 (2010).

[40] E. Gavartin, R. Braive, I. Sagnes, O. Arcizet, A. Beveratos, T. J. Kippenberg, and I. Robert-Philip, Optomechanical Coupling in a Two-Dimensional Photonic Crystal Defect Cavity, Phys. Rev. Lett. **106**, 203902 (2011).

[41] M. Zhang, S. Shah, J. Cardenas, and M. Lipson, Synchronization and Phase Noise Reduction in Micromechanical Oscillator Arrays Coupled Through Light, Phys. Rev. Lett. **115**, 163902 (2015).

[42] A. Mari, A. Farace, N. Didier, V. Giovannetti, and R. Fazio, Measures of Quantum Synchronization in Continuous Variable Systems, Phys. Rev. Lett. **111**, 103605 (2013).

[43] U. Akram, W. Munro, K. Nemoto, and G. J. Milburn, Photon-phonon entanglement in coupled optomechanical arrays, Phys. Rev. A **86**, 042306 (2012).

[44] J.-H. Gan, H. Xiong, L.-G. Si, X.-Y. Lü, and Y. Wu, Solitons in optomechanical arrays, Opt. Lett. **41**, 2676 (2016).

[45] H. Xiong, J. Gan, and Y. Wu, Kuznetsov-Ma Soliton Dynamics Based on the Mechanical Effect of Light, Phys. Rev. Lett. **119**, 153901 (2017).

[46] T. Kipf and G. S. Agarwal, Superradiance and collective gain in multimode optomechanics, Phys. Rev. A **90**, 053808 (2014).

[47] F. Bemani, R. Roknizadeh, and M. H. Naderi, Analog curved spacetimes in the reversed dissipation regime of cavity optomechanics, J. Opt. Soc. Am. B **34**, 2519 (2017).

[48] D. Bouwmeester, J.-W. Pan, K. Mattle, M. Eibl, H. Weinfurter, and A. Zeilinger, Experimental quantum teleportation, Nature (London) **390**, 575 (1997).

[49] A. K. Ekert, Quantum Cryptography Based on Bell's Theorem, Phys. Rev. Lett. **67**, 661 (1991).

[50] R. Dillenschneider, Quantum discord and quantum phase transition in spin chains, Phys. Rev. B **78**, 224413 (2008).

[51] O. F. Syljuåsen, Entanglement and spontaneous symmetry breaking in quantum spin models, Phys. Rev. A **68**, 060301(R) (2003).

[52] T. J. Osborne and M. A. Nielsen, Entanglement in a simple quantum phase transition, Phys. Rev. A **66**, 032110 (2002).

[53] G. D. Chiara and A. Sanpera, Genuine quantum correlations in quantum many-body systems: A review of recent progress, Rep. Prog. Phys. **81**, 074002 (2018).

[54] A. S. Sørensen, L.-M. Duan, I. Cirac, and P. Zoller, Many-particle entanglement with Bose-Einstein condensates, Nature (London) **409**, 63 (2001).

[55] J. Estève, C. Gross, A. Weller, S. Giovanazzi, and M. Oberthaler, Squeezing and entanglement in a bose-einstein condensate, Nature (London) **455**, 1216 (2008).

[56] K. Eckert, O. Romero-Isart, M. Rodriguez, M. Lewenstein, E. S. Polzik, and A. Sanpera, Quantum non-demolition detection of strongly correlated systems, Nat. Phy. **4**, 50 (2007).

[57] S. Chaudhury, S. Merkel, T. Herr, A. Silberfarb, I. H. Deutsch, and P. S. Jessen, Quantum Control of the Hyperfine Spin of a cs Atom Ensemble, Phys. Rev. Lett. **99**, 163002 (2007).

[58] T. Fernholz, H. Krauter, K. Jensen, J. F. Sherson, A. S. Sørensen, and E. S. Polzik, Spin Squeezing of Atomic Ensembles Via Nuclear-Electronic Spin Entanglement, Phys. Rev. Lett. **101**, 073601 (2008).

[59] D. Leibfried, B. DeMarco, V. Meyer, D. Lucas, M. Barrett, J. Britton, W. M. Itano, B. Jelenković, C. Langer, T. Rosenband, and D. J. Wineland, Experimental demonstration of a robust, high-fidelity geometric two ion-qubit phase gate, Nature (London) **422**, 412 (2003).

[60] K. Mølmer and A. Sørensen, Multiparticle Entanglement of Hot Trapped Ions, Phys. Rev. Lett. **82**, 1835 (1999).

[61] H. Müller-Ebhardt, H. Rehbein, R. Schnabel, K. Danzmann, and Y. Chen, Entanglement of Macroscopic Test Masses and the Standard Quantum Limit in Laser Interferometry, Phys. Rev. Lett. **100**, 013601 (2008).

[62] M. J. Hartmann and M. B. Plenio, Steady State Entanglement in the Mechanical Vibrations of two Dielectric Membranes, Phys. Rev. Lett. **101**, 200503 (2008).

[63] D. Vitali, S. Gigan, A. Ferreira, H. R. Böhm, P. Tombesi, A. Guerreiro, V. Vedral, A. Zeilinger, and M. Aspelmeyer, Optomechanical Entanglement Between a Movable Mirror and a Cavity Field, Phys. Rev. Lett. **98**, 030405 (2007).

[64] D. Vitali, S. Mancini, and P. Tombesi, Stationary entanglement between two movable mirrors in a classically driven fabry-perot cavity, J. Phys. A: Math. Theor. **40**, 8055 (2007).

[65] M. Paternostro, D. Vitali, S. Gigan, M. S. Kim, C. Brukner, J. Eisert, and M. Aspelmeyer, Creating and Probing Multipartite Macroscopic Entanglement with Light, Phys. Rev. Lett. **99**, 250401 (2007).

[66] L. Mazzola and M. Paternostro, Activating optomechanical entanglement, Sci. Rep. **1**, 199 (2011).

[67] S. Barzanjeh, E. Redchenko, M. Peruzzo, M. Wulf, D. Lewis, and J. Fink, Stationary entangled radiation from micromechanical motion, arXiv:1809.05865.

[68] R. Riedinger, A. Wallucks, I. Marinković, C. Löschnauer, M. Aspelmeyer, S. Hong, and S. Gröblacher, Remote quantum entanglement between two micromechanical oscillators, Nature (London) **556**, 473 (2018).

[69] C. F. Ockeloen-Korppi, E. Damskägg, J.-M. Pirkkalainen, M. Asjad, A. A. Clerk, F. Massel, M. J. Woolley, and M. A. Sillanpää, Stabilized entanglement of massive mechanical oscillators, Nature (London) **556**, 478 (2018).

[70] H. Ollivier and W. H. Zurek, Quantum Discord: A Measure of the Quantumness of Correlations, Phys. Rev. Lett. **88**, 017901 (2001).

[71] L. Henderson and V. Vedral, Classical, quantum and total correlations, J. Phys. A **34**, 6899 (2001).

[72] G. Adesso and A. Datta, Quantum Versus Classical Correlations in Gaussian States, Phys. Rev. Lett. **105**, 030501 (2010).

[73] P. Giorda and M. G. A. Paris, Gaussian Quantum Discord, Phys. Rev. Lett. **105**, 020503 (2010).

[74] T. Chanda, T. Das, D. Sadhukhan, A. K. Pal, A. Sen(De), and U. Sen, Emergence of entanglement with temperature and time in factorization-surface states, Phys. Rev. A **97**, 012316 (2018).

[75] F. Ciccarello and V. Giovannetti, Local-channel-induced rise of quantum correlations in continuous-variable systems, Phys. Rev. A **85**, 022108 (2012).

[76] V. Chille, N. Quinn, C. Peuntinger, C. Croal, L. Mišta, Jr., C. Marquardt, G. Leuchs, and N. Korolkova, Quantum nature of Gaussian discord: Experimental evidence and role of system-environment correlations, Phys. Rev. A **91**, 050301(R) (2015).